

# Relevance of Symmetry Assumptions in the 3D Numerical Modeling of a Flowformability Test

Nagasai Meghana Rani KAUTA<sup>1,a\*</sup>, Pierre-Olivier BOUCHARD<sup>1,b</sup>  
 and Katia MOCELLIN<sup>1,c</sup>

<sup>1</sup>CEMEF Mines ParisTech, PSL Research University, CNRS, UMR 7635, CS 10207 rue Claude Daunesse, 06904, Sophia-Antipolis Cedex, France

<sup>a</sup>nagasai.kauta@mines-paristech.fr, <sup>b</sup>pierre-olivier.bouchard@mines-paristech.fr,

<sup>c</sup>katia.mocellin@mines-paristech.fr

**Keywords:** flowformability test, finite element modeling, symmetry assumption

**Abstract.** A novel flowformability test is under development at CEMEF in order to be able to predict damage at large strains under complex loading conditions corresponding to tube flowforming. The design of this test relies on 3D numerical simulations performed with the finite element software Forge® 3.1 Nxt. Such simulations, using classical implicit updated Lagrangian formulations, are costly because of the very small-time step and the fine mesh required to describe accurately the local and evolving contact of the tube with the roller(s). The aim of this paper is to study the relevance and the influence of the use of symmetry conditions in the modeling accuracy of this flowformability test.

## Introduction

Flowforming process is a complex material cold forming process in which a preform of an initial thickness is deformed by the combining effect of a rotating roller and a mandrel until it reaches a desired final thickness value. A schematic set-up of a tube flowforming process is given in Fig.1. It is to be noted that tube flowforming is usually achieved with the use of 3 rollers placed at different longitudinal and radial positions.

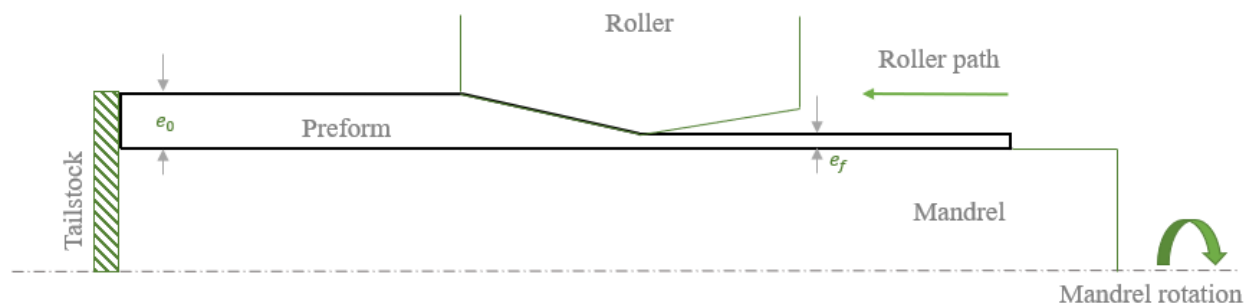


Figure 1: Schematic representation of a tube flowforming process

Input process kinematics which help in achieving the desired final preform geometry depend on the following important process parameters as reviewed in [1], [2]: feed ratio (defined as the ratio of roller feed velocity,  $v_{Roller}$  to mandrel rotational speed,  $\omega_m$ ), roller nose radius, roller path, roller attack angle and lubrication.

In such a complex process, for a given set of input process parameters, the material can reach large plastic strains, strain rates and alternating positive and negative stress triaxiality as seen in [3], [4]. It is difficult to characterize damage with standard characterization test as it occurs at very low values of deformation compared to flowforming. Thus, in order to characterize damage in the material, under such complex conditions, a suitable test is required.

A tube flowformability test has been demonstrated originally in [5] to characterize damage in the material during flowforming processes. As seen in Fig.2, the roller path is designed along an inclined plane. This allows a gradual increase in the thickness reduction ( $TR$ ) which is quantified as seen in Eq.1.

$$TR [\%] = \frac{e_0 - e_f}{t_0} \times 100 \quad (1)$$

Maximum thickness reduction ( $TR_{max}$ ) is the value of  $TR$  such that the final thickness,  $e_f$  reaches a critical value,  $e_c$ , where damage is visible during the test. In [5], the authors evaluated an approximative function between  $TR_{max}$  as a function of the process parameters. This is a method to understand the relation between the process parameters and the occurrence of damage as a function of  $TR$ . A similar classical test configuration is seen in [6], [7] with a hybrid computational-experimental approach in characterizing damage by means of  $TR$ .

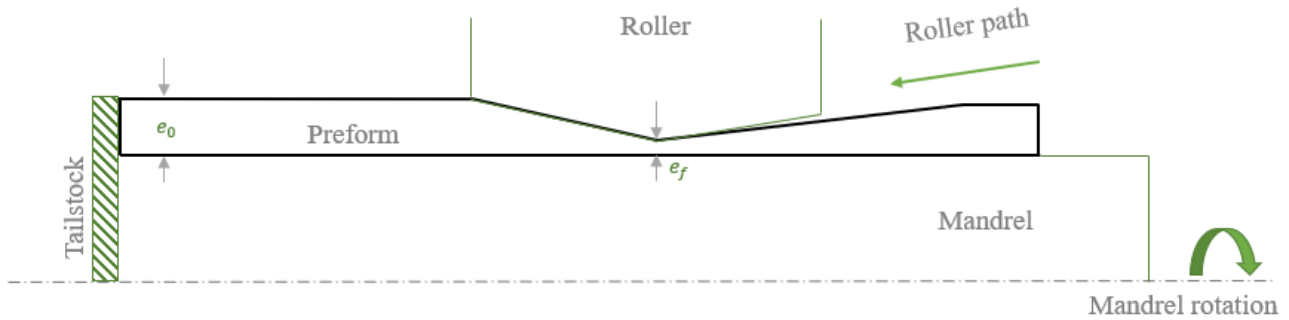


Figure 2: Schematic representation of a classical tube flowformability test

3D flowforming process simulations are not cost efficient. This makes it challenging to optimize the process over a wide range of process parameters. [8], [9] introduce geometrical reductions by symmetrical considerations in their models to increase the cost efficiency. It is seen that the roller forces are accurately predicted and computational costs are significantly reduced by the introduction of the symmetrical planes. However, localized material response is compromised in both [8], [9], since tube flowforming does not allow such symmetry conditions.

As part of the current study, the design of a novel flowformability test is introduced with a new roller path, mandrel and preform designs unlike the classical flowformability tests seen in the literature. An equivalent 3D computational model of the test is designed which is used to analyze damage that is seen in the real test<sup>1</sup>. Since the computational cost of this reference 3D model is observed to be much higher, two geometrical reductions using symmetrical planes are introduced and their reliability is evaluated with respect to the preform profile, roller forces and localized deformation results. In a 2D simulation the deformation of the preform in the plane of mandrel rotation is neglected. Hence, it is not analyzed as part of this study.

### Novel Flowformability Test

The flow formability test being developed is a reformed version of the tube flowformability test (also called tube spinnability test) found in the literature. Due to machine limitations at CEMEF, roller movement is restricted only to move in the horizontal direction, parallel to the mandrel axis (z). In order to induce an increasing  $TR$ , it is therefore not possible to move the rollers in the radial direction.  $TR$  is induced by using an angular tube as a preform with a 2° wedge angle. As seen in Fig.3, this preform is placed on a rotating mandrel. In test conditions, three rollers are used- the “Roller C” primarily induces  $TR$  while the supplementary rollers minimize the fluctuations of the mandrel-preform system and maintain stability.

The objective of this test design is to characterize damage using a hybrid experimental-computational approach as seen in [6], [7]. Therefore, an equivalent 3D computational model that is designed, is discussed in the next section.

<sup>1</sup> Damage characterization and the results of the real test to be presented in future work

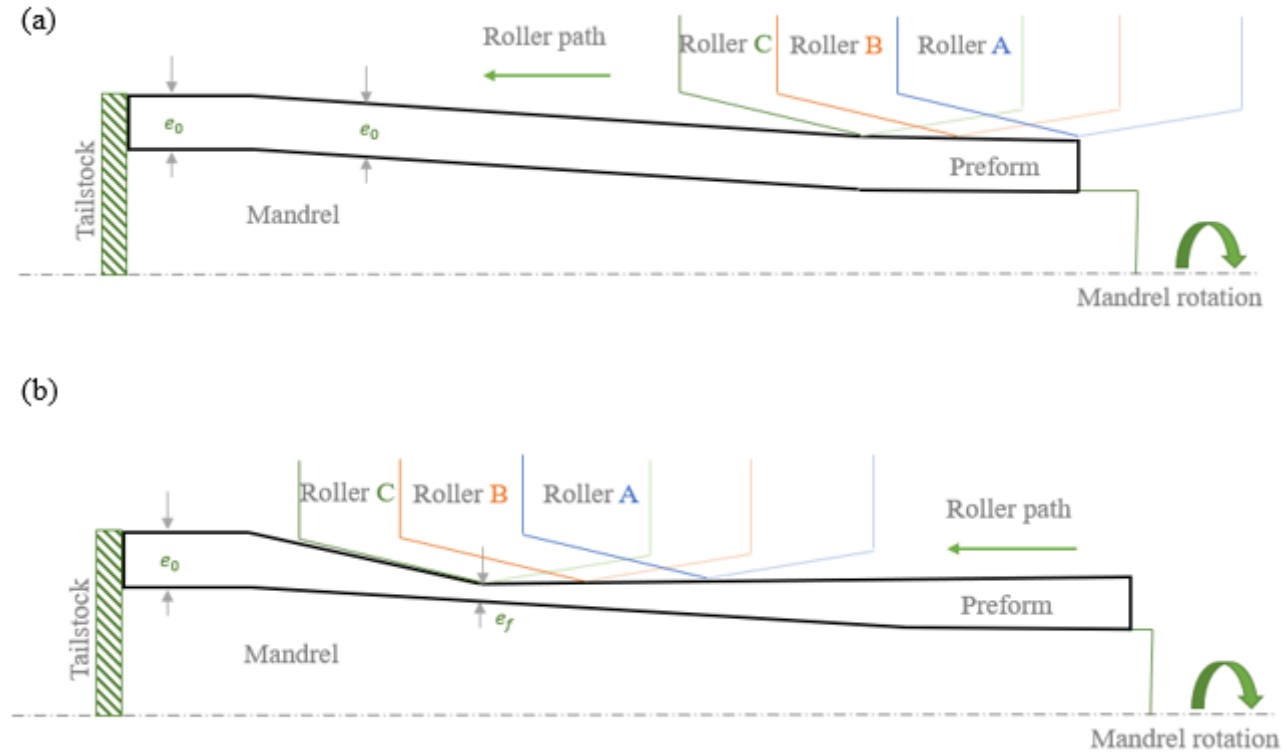


Figure 3: Schematic representation of the novel flowformability test- (a) initial (b) intermediate configuration

### Flowformability Test Simulations

The flowformability test is simulated using 3D computational model based on classic Lagrangian approach in Forge® 3.1 Nxt software. In the model, the roller and the mandrel are rigid bodies and the mandrel-preform system is stable unlike in a real test. Therefore, the model set-up is simplified in comparison with the real test by using only the principal attacking roller (Roller C) as seen in Fig.4(a). This test is performed at room temperature and the process parameters are as seen in Table 1.

This test is planned to be performed on Al6061 material preforms. The geometry of these preforms is seen in Fig.4(b). The material behaviour law represented by relation between equivalent stress,  $\sigma_{eq}$  and equivalent strain,  $\bar{\epsilon}$  is given by Hollomon power-law,  $\sigma_{eq} = K\bar{\epsilon}^n$ . The parameters of this law (Bulk Modulus,  $K = 216.45$  MPa; strain hardening exponent,  $n = 0.18$ ) are identified using a compression test. The Coulomb friction model limited by Tresca criterion is used between the mandrel and the preform with the friction coefficient,  $\bar{m} = 0.4$ . Unilateral sliding is considered between the roller and the preform. The preform is meshed using three zones of mesh sizes. The ratio of the smallest to the largest mesh size used is 0.2. The mesh zone distribution can be seen in Fig.5.

In this study, two configurations called “120°” and “90°” are designed in addition to the reference 360° configuration. In these configurations, the preform geometry is reduced circumferentially such that it forms 120° and 90° angular sectors in the plane-xy as seen in Fig.6 (b) and (c) respectively. Two symmetry planes, as indicated, are introduced on the lateral edges of the preform in order to facilitate this geometry. All process parameters, material and friction behaviour, mesh distribution and temperature are maintained the same in these configurations as in the 360° one.

This is intrinsically a non-symmetrical test. Based on the works presented in the literature, it is assumed that models with symmetry planes are capable of reproducing similar results as in the reference 360° configuration. One of the objectives of this study is to verify this assumption by comparing the results of the three configurations.

Table 1: Process parameters

Parameter	Value
Roller attack angle, $\alpha_r$ [°]	20
Initial thickness of preform, $e_0$ [mm]	5
Feed ratio, $f$ [mm/r]	0.39

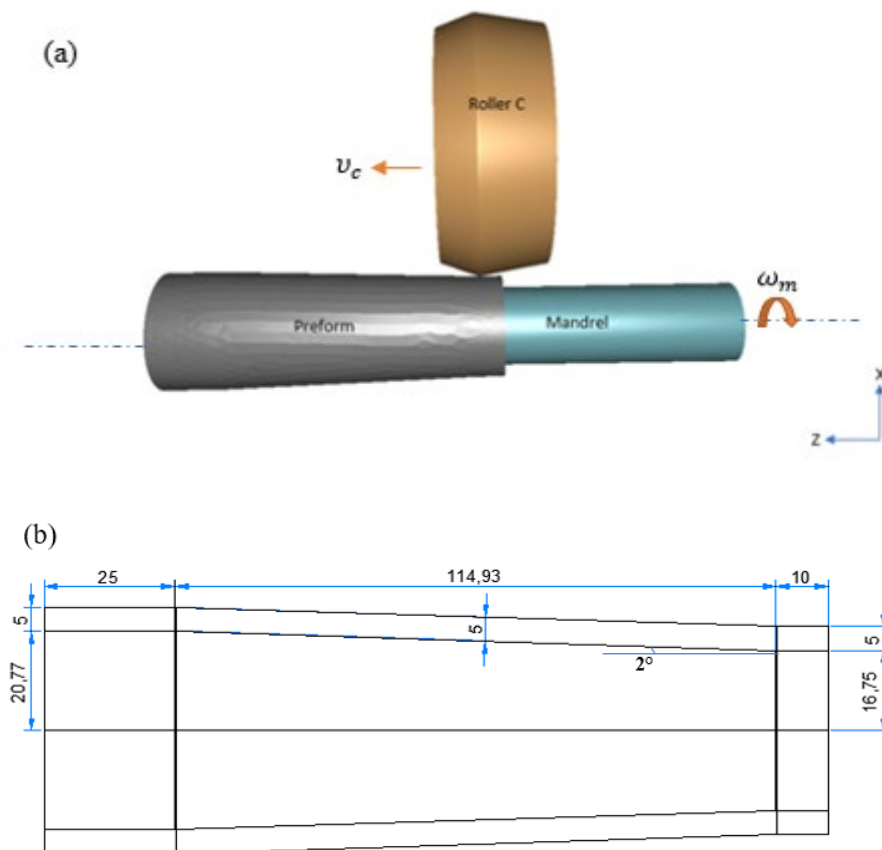
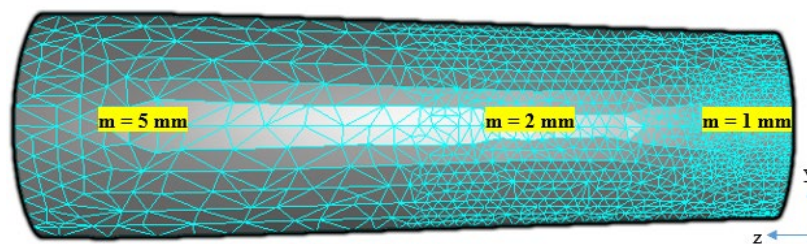
Figure 4: (a) Flowformability test set-up (b) Preform geometry<sup>2</sup>

Figure 5: Mesh size distribution in test preform

<sup>2</sup> All dimensions are in millimeters (mm)

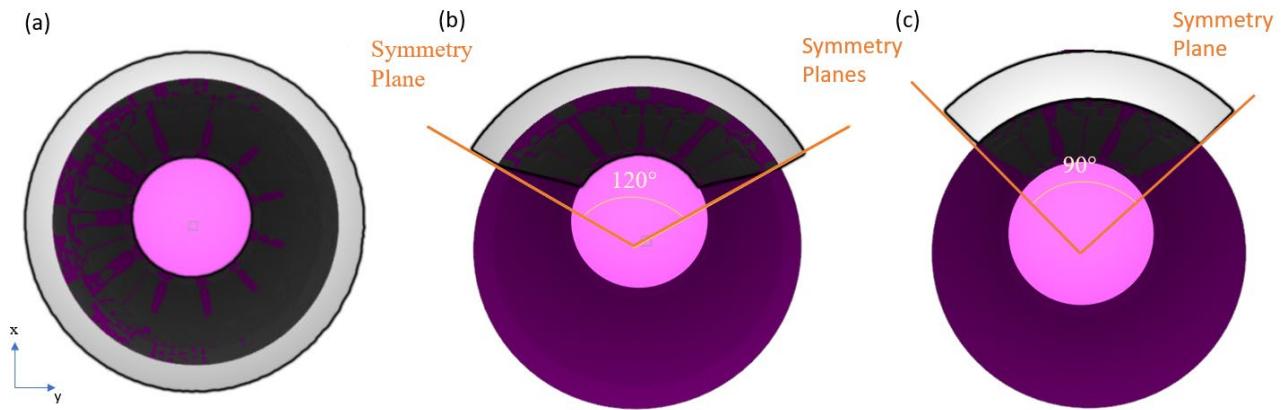


Figure 6: Preform geometries in (a) 360°, (b) 120° and (c) 90° configurations

## Results

In this section, the relevance of the two symmetry configurations is analyzed by comparing their results with the reference 360° configuration.

### *CPU Time*

In all three cases, the computations are launched on 6 CPUs of a calculation computer<sup>3</sup>. As expected from the implementation of symmetry planes, the computational cost is much lesser in the symmetrical configurations compared to the 360° configuration. The computational costs shown in Table 2 correspond to the three cases until process time of 40s<sup>4</sup>.

Table 2: CPU Time until process time of 40s

Configuration	Number of elements	CPU Time
90°	14392	1.22 days
120°	17940	1.88 days
360°	34861	6.63 days

### *Roller Forces*

The radial and axial roller forces are seen in Fig.7. The evolution of forces in the 120° and 90° configurations are comparable to the tendency of the 360° configuration until 40s. After 40s, the two simplified configurations tend to underestimate the forces, but the difference remains very small.

### *Preform profile*

A cutting plane is introduced in the plane-xz which allows the analysis of the evolution of the preform profile in the three cases. As seen in Fig.8, the preform profile of the “symmetry” configurations are representative of the “reference” configuration until 40s. A debonding is observed in the form of a material flow at 40s. This flow increases at 60s and is different in the three configurations. This can explain the difference in the roller forces between the three cases, after 40s, as seen in Fig.7.

### *Equivalent strain*

Distribution of equivalent plastic strain of the three configurations is seen along the length and thickness of the preform profile section in plane-xz and at process time of 40s in Fig.9. It is observed that the configurations with symmetry plane underestimate the equivalent strain at the surface closer to the roller side of the preform.

<sup>3</sup> CPU : Intel(R) Xeon(R) CPU E5-2630 v3 @ 2.40 GHz

<sup>4</sup> s: seconds

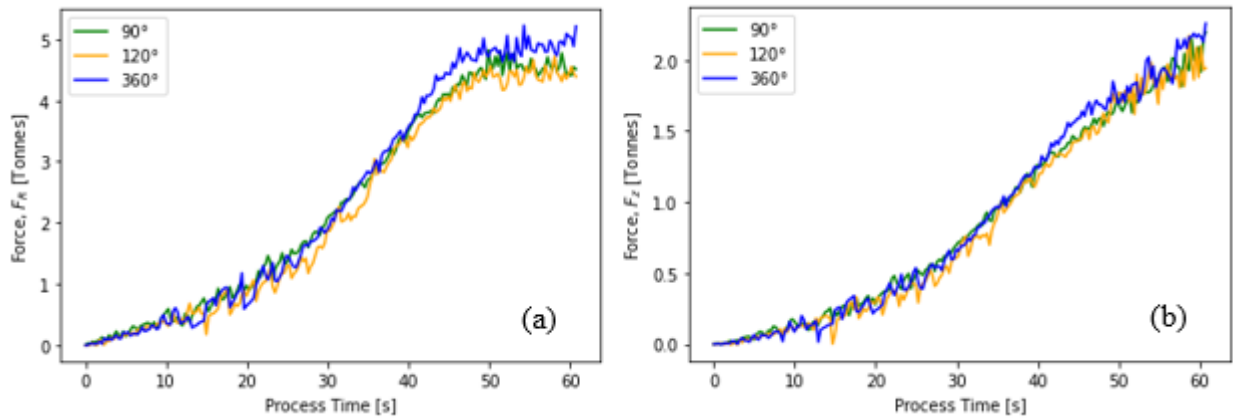


Figure 7: Roller forces in the (a) radial and (b) axial, z directions until process time of 60s

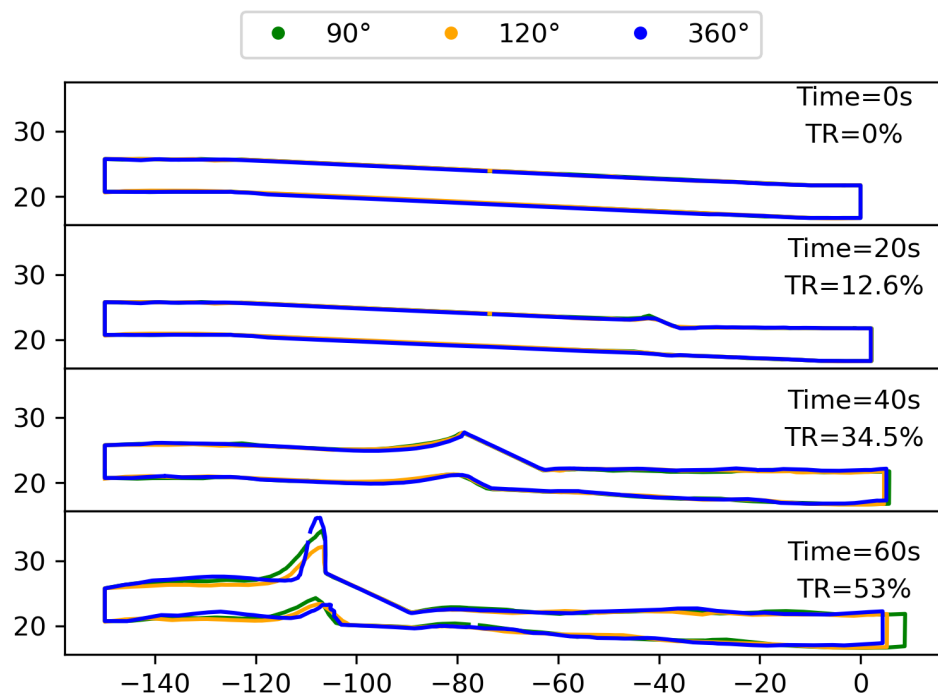


Figure 8: Preform profile in plane-xz at different process times

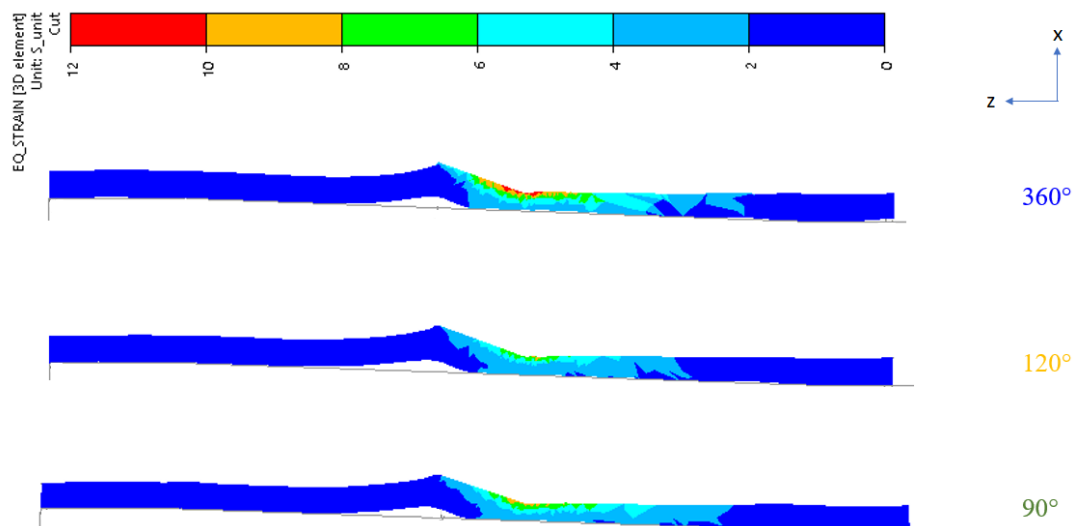


Figure 9: Equivalent plastic strain distribution in a cut-section in plane-xz at process time of 40s

## Discussion

An increasing thickness reduction,  $TR$  is achieved using the novel flowformability test during the process time as seen in Fig.8. The definition of  $TR$  is given in Eq.1. With the given process parameters, material and friction law inputs and mesh conditions, the  $360^\circ$  case shows that the preform can reach localized plastic strain of up to 12 at 34.5%  $TR$  as seen in Fig.9. Thus, this test design allows to reach large deformation values as is seen in the classic flowformability test.

Since, the simulation with  $360^\circ$  configuration takes more than 6 days to complete, two simplified configurations with symmetry planes are introduced and their comparison in terms of local and global results is demonstrated. It is evident that the configurations with symmetry planes reduce computational costs significantly as seen in Table 2. However, their reliability needs to be evaluated in modeling such a non-symmetric test. Roller forces in axial and radial directions obtained using  $120^\circ$  and  $90^\circ$  configurations are representative when compared to the  $360^\circ$  case until process time of 40s. From 40s to 60s of process time, there is a slight difference between the roller force values obtained. This may be attributed to the observation in Fig.8 that there is an apparent debonding from 40s to 60s. The debonding observed can be influenced by a multitude of factors including friction coefficient considered between the mandrel and preform, roller attack angle in addition to others. The associated pile-up of material is also difficult to model and to mesh. Some discrepancies between the models can also come from some distortion of the mesh.

## Conclusion

A novel flowformability test is presented with three different preform configurations models. The following are the main conclusions of this study:

- The CPU cost of  $90^\circ$  case is nearly one -sixth times that of  $360^\circ$  case until a process time of 40s.
- The roller forces and preform geometry in the three configurations are representative of each other as long as there is no debonding between the preform and the mandrel.
- Possible factors for the occurrence of debonding are discussed. A real experiment is necessary in order to evaluate friction parameters and validate the possibility of the material flow as seen in the model. The use of three rollers in the flowforming experiment (instead of one here) may have a beneficial effect on the reduction of the observed numerical material pile-up.
- Localized equivalent plastic strains vary when compared among the three cases. The configurations with symmetry planes tend to underestimate these localized strains values when compared to the reference  $360^\circ$  case.

In conclusion, the simulations with symmetrical configuration  $90^\circ$  -with the least CPU time- can be used as long as the global results such as forces on the tools and preform profile are analyzed. These configurations are not reliable where there is debonding or material flow. Furthermore, they underestimate the level of equivalent plastic strain and their use for the prediction of formability is dangerous. Symmetry planes can therefore be used for reducing the CPU time when calibrating the tube flowformability process parameters. Once they are determined, it is recommended to perform simulations using full  $360^\circ$  configurations in order to analyze local stress-strain data for the prediction of ductile fracture.

The study of damage characterization of the new flowformability test is dependent on a real test. The current study is limited to a discussion of an overview of the modeling of a new flowformability test and the reliability of two configurations with symmetry planes. This study will be extended to pursue damage characterization analysis in a future work.



---

**References**

- [1] O. Music, J. M. Allwood, and K. Kawai, A review of the mechanics of metal spinning, *J. Mater. Process. Technol.*, vol. 210, no. 1, pp. 3–23, 2010.
- [2] C. C. Wong, T. A. Dean, and J. Lin, A review of spinning, shear forming and flow forming processes, *Int. J. Mach. Tools Manuf.*, vol. 43, no. 14, pp. 1419–1435, 2003.
- [3] M.-A. Vidal, P.-O. Bouchard, K. Mocellin, et al., Étude numérique et expérimentale du procédé de fluotournage cylindrique de tubes, in *Colloque MECAMAT*, Aussois, France, 2019.
- [4] O. I. Bylya, T. Khismatullin, P. Blackwell, and R. A. Vasin, The effect of elasto-plastic properties of materials on their formability by flow forming, *J. Mater. Process. Technol.*, vol. 252, pp. 34–44, 2018.
- [5] S. Kalpakcioglu, Maximum Reduction in Power Spinning of Tubes, *J. Eng. Ind.*, vol. 86, no. 1, pp. 49–54, 1964.
- [6] H. Ma, W. Xu, B. C. Jin, D. Shan, and S. R. Nutt, Damage evaluation in tube spinnability test with ductile fracture criteria, *Int. J. Mech. Sci.*, vol. 100, pp. 99–111, 2015.
- [7] W. Xu, H. Wu, H. Ma, and D. Shan, Damage evolution and ductile fracture prediction during tube spinning of titanium alloy, *Int. J. Mech. Sci.*, vol. 135, pp. 226–239, 2018.
- [8] A. M. Roula, K. Mocellin, and P.-O. Bouchard, Numerical Modelling of the Flow Forming Process: Computation Time Optimization and Accuracy Analysis, in *ICTP 2021*, Online, United States, 2021, pp. 493–506.
- [9] E. Sariyarlioglu, Analysis of tube spinning process. M.Sc Thesis, Istanbul Technical University, 2021.